Microtubule Dissassembly In Vivo: Intercalary Destabilization and Breakdown of Microtubules in the Heliozoan *Actinocoryne contractilis*

Colette Febvre-Chevalier and Jean Febvre

Laboratoire de Biologie Cellulaire Marine URA 671 C.N.R.S., Observatoire Océanologique de Villefranche-sur-Mer, 06230, France and Laboratoire de Biologie et Physiologie Cellulaires Marines, Faculté des Sciences, Université de Nice, 06034, Nice-Cedex, France

Abstract. In the marine heliozoan *Actinocoryne contractilis*, uninterrupted rods of microtubules stiffen the axopodia and the stalk. Stimulation in sea water elicits an extremely fast contraction (millisecond range) accompanied by almost complete Mt dissociation. Using high-speed cinematography and light transmittance measurements, we have studied the process of Mt disassembly in real time. In sea water, Mt disassembly follows an exponential decrease (mean half time of 4 ms) or proceeds by short steps. Cell contraction and Mt disassembly have been inhibited or slowed down through the use of artificial media. Although kinetics are slower (mean half time of 3 s), the curves of the length change against time look similar. The rapid as well as the slower process are accompanied by the formation of breakpoints on the stalk, from which disassembly proceeds. In specimens fixed during the slowed contraction, the presence across the Mt rods, of a single or multiple destabilization band that may consist of granular material and polymorphic forms of tubulin supports the hypothesis of "intercalary destabilization and breakdown" of axonemal Mts.

SEVERAL schemes have been suggested to explain the way in which microtubule assembly and disassembly can be brought about. One of the first models proposed that subunits may be exchanged along the whole length of the microtubules (Mts)[1] (Inoué and Sato, 1967; Inoué and Ritter, 1975). Later, on the basis of biochemical data, the assembly-disassembly process was interpreted as the result of an equilibrium between microtubule-polymers and a critical concentration of tubulin subunits at steady state (Johnson and Borisy, 1977). The role of GTP was defined (Carlier and Pantaloni, 1981) showing that the Mts with terminal bound GTP subunits (GTP caps) are more stable than those uncapped (terminal guanosine diphosphate [GDP] subunits) (Carlier, 1982). These data, and the behavior of individual Mts in a solution of tubulin (catastrophic disassembly), suggested a GTP cap model for dynamic instability (Mitchison and Kirschner, 1984). However, Mt kinetics is sometimes so fast that a breakdown and annealing hypothesis was suggested to account for rapid remodeling of microtubules (Salmon, 1984).

The present paper is focused on a remarkably rapid disassembly of Mts in the stalked heliozoan *Actinocoryne contractilis*. The first ultrastructural evidence for a Mt-based cytoskeleton in the heliozoans was provided by Tilney and Porter (1965). It was then suggested that the microtubule rods in these microorganisms were involved in elongation and shortening of long stiff processes, the axopodia (Tilney and Porter, 1967). We report experiments which suggest that "intercalary destabilization and breakdown of Mts" may be one of the systems used in vivo by heliozoans for the very rapid shortening of the axopodia and the stalk. The present paper deals only with the extremely rapid process of Mt disassembly, not the mechanism of force production involved in cell contraction.

1. *Abbreviations used in this paper*: Am, artificial media; DB, destabilization bands; GDP, guanosine diphosphate; Mt, microtubule; NMG, *N*-methyl-glucamine; PEGc, polyethylene glycol compound; SW, sea water.

Materials and Methods

Sampling and Preparations of the Living Material

Large vegetative specimens of *A. contractilis* were collected in the bay of Villefranche-sur-Mer, near Nice (France) in shallow water (8–15 m) from solid substrata. After isolation of the specimens under a stereomicroscope, they were cultured at 14–18°C in filtered sea water (SW) and were fed with oligotrich ciliates.

For light microscopy experiments and fixation, the specimens were manipulated individually. They were attached horizontally on a slide with a very small dab of VALAP (1:1:1 mixture of vaselin, lanolin, paraffin). The coverslip was adjusted at convenient height with VALAP and solutions were perfused through this chamber with a syringe.

Observation of Living Specimens and Recording Techniques

The preparations were viewed with a Jenalumar (Jenaval), Ortholux or Orthoplan (E. Leitz, France) light microscope equipped with a Nomarski interference contrast system or with polarizing optics. Three recording techniques were used.

High speed 16-mm color films (4,000–8,000 fr/s) were made with a

Hitachi camera coupled to a Orthoplan microscope (brightfield or Nomarski contrast system, obj 25 or 40). Illumination was provided by a xenon lamp supplied with stabilized current. Eastman Kodak color reversal 400 ASA developed at 800 ASA was used throughout. Sequences were analyzed on a mounting table at final magnifications ×375 or ×600. The outline of the stalk and head was transferred to tracing paper from successive frames. High speed cinematography showed the rapid contraction in real time. It allowed us to plot the length change against time directly from the frames. It is thus regarded as the reference method. The curves were plotted with "Cricket Graph" program (Cricket Software, 1988).

Changes in the length during contraction were also recorded as changes in the light transmittance via a photodiode (Photops UDT 455 supplied by United Detector Technology, Hawsthome, C. 90 250) coupled with a 5103 N storage oscilloscope (Tektronix, S.p.A., Milan, Italy). The best sensitivity of the photodiode was at 550 nm. To increase signal/noise, interference color contrast was adjusted to produce a yellow specimen on a blue background A split field diaphragm was used to limit the light on either sides of stalk and head. A DC light source was necessary to avoid AC interference. Since the diameter of the head and the width of the stalk are almost unchanged during contraction, the variation of area was a direct function of the length variation. The spatial resolution was 10 μm for the 25× and 6 for the 40× objective lenses. The temporal resolution was 0.2 ms. This system gave accurate measurement of the duration of contraction but requires slight adjustments to fit exactly with the kinetics from high speed films.

The slow contractions induced in artificial media were recorded through a color UMATIC 3/4 inch Video system (Sony Magnetoscope VO 5630; Sony (Montvale, NJ) coupled to a CCD camera (Sony 101 P) and a high definition monitor (Trinitron Sony Monitor PVM).

Stimulation

Mechanical stimuli were given with a glass microneedle attached to a loud speaker diaphragm. For electrical stimulation, a specimen was placed between two platinum or silver electrodes 5-mm apart and 2–5 ms, 10 V pulses given from a home-built stimulator. In both cases, the stimuli were arranged to trigger the oscilloscope.

Artificial Media

Before experiments the specimens were rinsed with artificial sea water (ASW). The basic composition of ASW was 500 mM NaCl, 58 mM $MgCl_2$ or $MgSO_4$, 10 mM $CaCl_2$, and 10 mM KCl adjusted to pH 8.0 with Tris(hydroxymethyl)2-4 aminoethane-hydrochloride (Tris-HCl) or Pipes (Sigma, France).

The following artificial media (AMs) were used to obtain complete stabilization or mild destabilization of the Mt arrays: (*a*) Deuterium oxide (D_2O) (Merck, Darmstadt) was substituted for H_2O up to 60% in ASW. (*b*) Ca^{2+}-EGTA buffers containing: 500 mM Tris, 10 mM KCl, 2–10 mM $MgSO_4$, ethylene-glycol-bis(aminoethylether)*N*,*N*'-tetraacetic acid (EGTA) 0.2–10 mM, polyethylene glycol compound (PEGc), 0.1–1 mM (Sigma, France). pH adjusted to 6.8–8.0. *N*-methyl glucamine (NMG) or sucrose plus Pipes could also be used instead of Tris. Ca^{2+}-free concentration was calculated from Chang et al. (1988), and (*c*) inhibitors of Ca^{2+} fluxes were also used such as caffeine (10 mM), theophylline (1–10 mM), and quercetine (50–100 μM dissolved in methanol ⩽1%) (Sigma, France).

Preparations for Electron Microscopy

The specimens were either fixed directly without any preliminary treatment or after complete stabilization or mild destabilization in AMs. Fixations were either carried out as reported previously (Febvre-Chevalier, 1980) or according to the protocol of de Brabander and co-workers (1976) modified as follows: after rinsing the protozoan for 2–10 min in the AMs at room temperature, it was fixed in a mixture of formaldehyde and glutaraldehyde (final concentrations 2 and 2.6% respectively) in phosphate buffer (0.2 M final concentration) (pH 7.4) at room temperature for 15 min. Then, it was transferred directly into a mixture of glutaraldehyde (2% final) in sodium cacodylate (0.37 M) and osmium tetroxide (1% final) in veronal acetate (0.05 M) for 1 h at 5°C. For fixing the specimen in the completely stabilized state, 10 mM EGTA was added into the fixative. After staining with 0.5% uranyl acetate (40 min) it was rinsed in cacodylate buffer during 1 h, dehydrated in ethanol, and embedded in Spurr resin or Epon 812. Ultrathin sections were stained with uranyl acetate and lead citrate before examination in an electron microscope (H600; Hitachi Ltd., Tokyo).

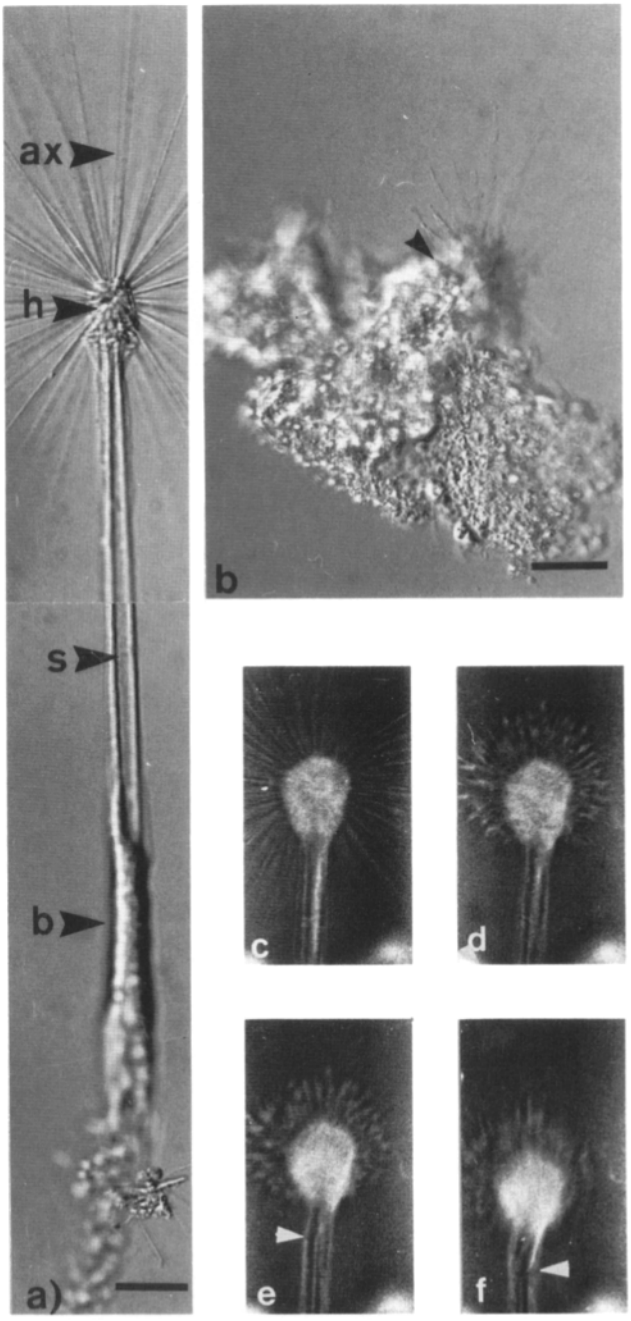

Figure 1. Light microscopical views of *A. contractilis* in natural SW. (*a*) Fully extended single-stalked specimen showing the cytoplasmic base (*b*) attached on the surface of a Thermanox microslide, the stalk (*s*) and the head (*h*) surrounded by numerous axopodia (*ax*). (*b*) Contracted specimen showing the flat base attached to the substratum. The head and the axopodia are just reforming (*arrowhead*). (*c–f*) Frames from a high speed film at 4,600 fr/s, showing the rapid contraction in natural SW after electrical stimulation. (*c*) The specimen prior to contraction; (*d*) the axopodia are beginning to shrink; (*e*) and (*f*) the stalk folds down (*arrowheads*) while contracting suggesting the breaking of the axonemal rods. Time interval between successive frames: 0.6 ms. Bars: (*a* and *b*), 30 μm.

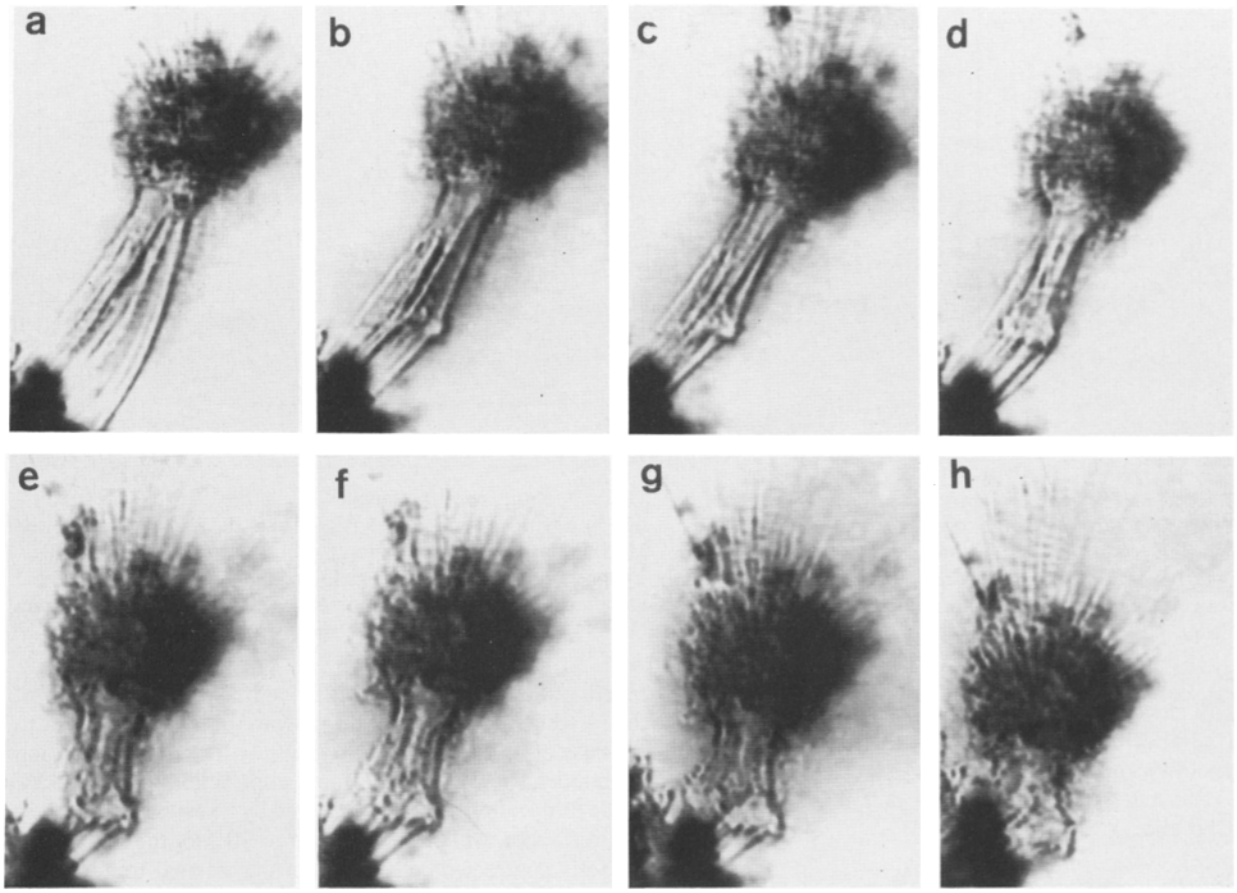

Figure 2. Series of frames from a video-recording (25 fr/s) showing the slowed contraction elicited in quercetine, 100 μM in ASW. The frames are at 1-s intervals. (*a*) The specimen before contraction. (*b–d*) A bulge appears on the stalk at the level of one rod and then progresses to the next ones. (*e–h*) folding and shortening of the stalk proceeds from this region. Bar, 150 μm.

Results

The heliozoans are generally free-living single cells having a spherical cell body from which long slender axopodia radiate. Axopodia, supported by Mt-arrays (axonemes), arise from one or several microtubule organizing centers (MTOC). In contrast, the stalked species *Actinocoryne contractilis* shows a polarity of the cell body. It consists of a head (30–70 μm in diameter) including a large MTOC, surrounded by hundreds of axopodia (50–500-μm long), linked to a flat base by a long single stalk (50–800-μm long, 5–20-μm thick) which is stiffened by a few large axonemes (Febvre-Chevalier, 1980) (Fig. 1, *a* and *b*). The cell membrane is highly excitable (Febvre-Chevalier and Febvre, 1981), and the response to diverse stimuli is an overshooting Na^+- and Ca^{2+}-dependent action potential (Febvre-Chevalier et al., 1986). Subsequently, a complete contraction occurs which is several orders of magnitude faster than in any other microtubule based system (Fig. 1, *c–f*) (Febvre-Chevalier, 1981; Febvre-Chevalier and Febvre, 1986).

Effect of the Artificial Media on the Contractile Behavior

Different media were used to obtain a complete or partial destabilization of the Mt cytoskeleton (Fig. 2).

In D_2O (up to 60%) containing ASW the rapid contraction could be abolished and the Mt cytoskeleton was stabilized provided that incubation lasted more than 1 h. Below this delay a rapid or slightly slowed contraction generally occurred.

Ca^{2+}-EGTA buffers allowed us to determine the threshold concentration of Ca^{2+} in which either response was obtained. The standard incubation time was 10 min.

Below the Ca^{2+} concentration of 4.10^{-9} M in Ca^{2+}-EGTA buffers, 100% of the specimens were totally inhibited and unable to perform contraction whatever the stimulation.

In the range of 4.10^{-9}–10^{-7} M, the response was either a slow contraction (6–15 s) (64% of the cases), a complete stabilization (23% of the cases) or a rapid contraction (13% of the cases).

In the range of 10^{-7}–10^{-6} M, the response was a rapid contraction (67%), a slow contraction (27%), or a complete stabilization (6%).

Above 10^{-6} M the rapid contraction was always triggered as in SW or ASW.

As soon as the destabilization was triggered it progressed until the end of the contraction. PEGc may contribute to stabilization in Ca^{2+}-EGTA buffers around the threshold concentration of 10^{-7} M.

Inhibitors of Ca^{2+} fluxes (caffeine, quercetine) added into

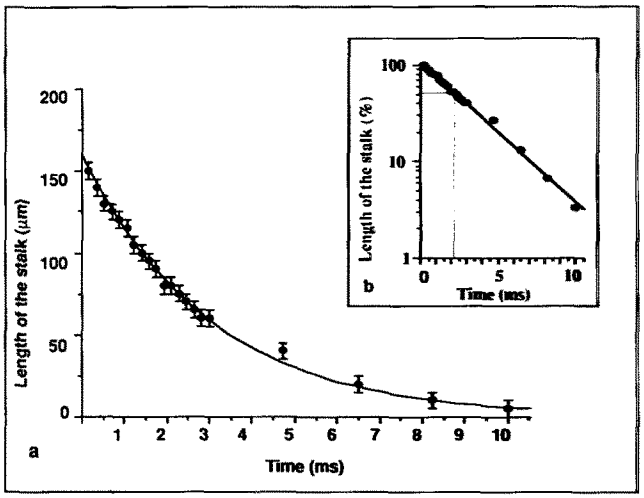

Figure 3. Example of the kinetics of a rapid contraction in SW from a high speed film (4,800 fr/s). Exponential fit: 0.995. (*a*) Length change plotted against time of a single-step rapid contraction which shows the extremely rapid Mt destabilization. (*b*) Semilogarithmic scale. Halftime = 2.2 ms.

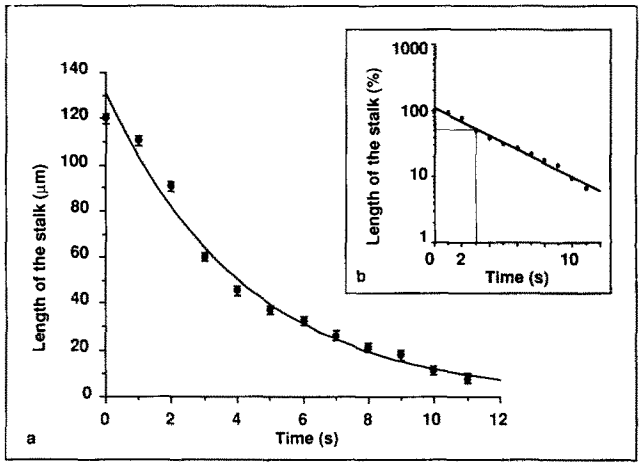

Figure 5. Example of the kinetics of a slowed single-step contraction in AM from a video recording. The trace suggests that slowed Mt destabilization follows smooth decreasing exponential kinetics. Exponential fit: 0.987. (*a*) Tracing of the decreasing exponential variations of length as a function of time. Duration of the contraction: 11 s. (*b*) Semilogarithmic scale. Halftime: 3 s.

SW or ASW slowed the contraction as previously described (Febvre-Chevalier and Febvre, 1986). In the presence of Ca^{2+} channel blockers (Mn^{2+}, Co^{2+}, La^{3+}) the rapid contraction was replaced with a slowed and delayed contraction (Febvre-Chevalier et al., 1986).

Kinetics of the Contraction

Kinetics of the rapid contraction elicited in natural SW by mechanical and electrical stimuli were examined with high speed cinematography (Febvre-Chevalier and Febvre, 1981, 1986) and by light transmittance measurements. Cinerecordings showed that the axopodia and the stalk fold down and proceeded by steps during the rapid contraction (Fig. 1, *c–f, arrowheads*) or shortened with a smooth motion. The mean length of the specimens selected for studying the kinetics of the rapid contraction (measured from the top of the head to the base of the stalk) was 185 μm (n = 20). Both recording techniques showed that the rapid contraction involves 80% of the total cell length. It is followed by a very slow cytoplasmic retraction which corresponds to 10% of the length and the fully contracted cell is 10% of the original total length. The rapid contraction develops within 4–20 ms, corresponding to a contraction velocity of 1–6 cm · s^{-1} or 50–300 lengths · s^{-1}. Since contraction involves at least 90% of the initial length (168 μm for a mean initial length of 185 μm; half length 84 μm), mean half time for contraction is 4 ms. The curves of the length plotted against time are smooth decreasing exponentials (Fig. 3) or proceeds by short steps (Fig. 4).

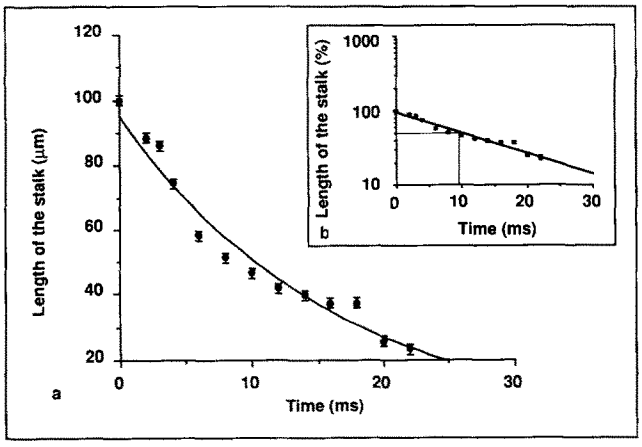

Figure 4. Example of the kinetics of a stepwise rapid contraction in SW from a high-speed film at 4,800 fr/s suggesting breaks in the axonemes during the rapid Mt destabilization. Exponential fit: 0.962. (*a*) Linear scale showing three steps of the quasi exponential decrease. Contraction is completed within 22 ms. (*b*) Semilogarithmic scale showing that the points delineate a series of exponential steps. Halftime: 10 ms.

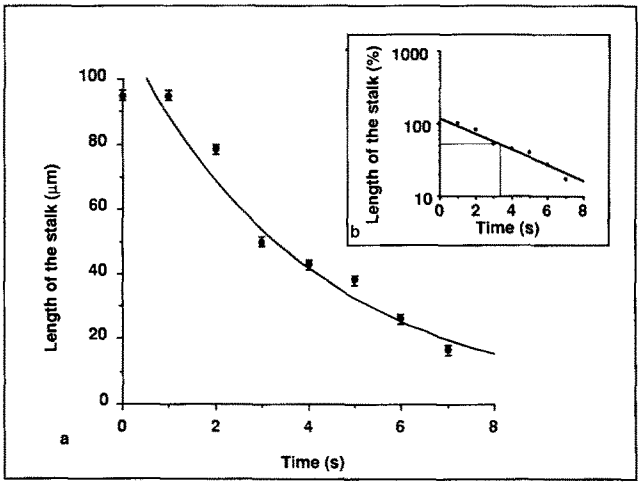

Figure 6. Example of the kinetics of a slowed multiple-step contraction in AM from a video recording suggesting the presence of breaks during the Mt destabilization. Exponential fit: 0.958. (*a*) Tracing of the stepwise decrease of length during the slowed contraction. Contraction duration: 7 s. (*b*) Semilogarithmic scale. Half time: 3.2 s.

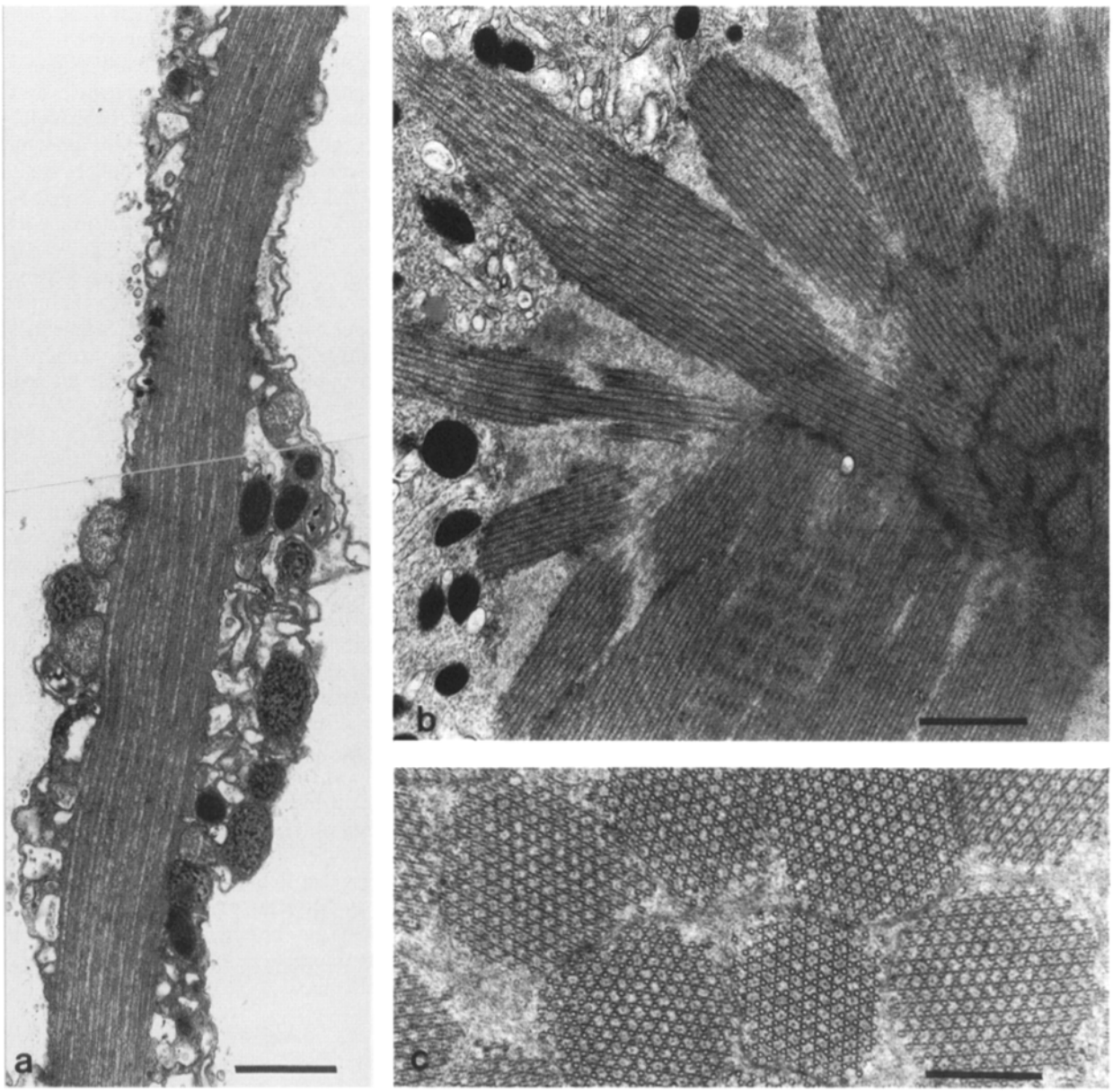

Figure 7. Thin sections through the axonemal complex after complete stabilization for 10 min in Ca^{2+}-EGTA containing 500 mM Tris, 2 mM $MgSO_4$, 10 mM KCl, 1 mM PEGc, 5 mM EGTA, pH 8.2. To prevent retraction at the fixation, 10 mM EGTA was added into the fixative. (*a*) Longitudinal thin sections through the stalk of a single stalked specimen. (*b*) Longitudinal section through the head close to the MTOC showing the axonemes oriented radially towards the axopodia, longitudinally towards the stalk. (*c*) Cross section through axonemes in the head showing the hexagonal Mt pattern. Bars: (*a* and *b*) 1 μm; (*c*) 0.5 μm.

Slow contraction could be elicited in AMs as described above. It was generally jerky, proceeding in two or three steps. A thickening resembling a knee appeared at any place along the stalk from which the slow contraction propagated (Fig. 2). As for the rapid contraction, the curves of the length change versus time are either smooth decreasing exponentials (Fig. 5) or stepwise (Fig. 6) but the half time is around 3 s. Duration of the slower contraction is around 10 s.

Mt Arrays after Complete Stabilization

After complete inhibition of the contraction, the Mt bundles appeared to be stabilized and the birefringence of the Mt arrays was conserved. Thin sections showed that the cytoplasm was well preserved and the Mts were undamaged as shown in Fig. 7, *a–c* and detailed below.

The axopods, head and stalk are supported by several hundreds of patterned arrays of Mts that arise from a large MTOC located in the center of the head (Fig. 7 *b*). This MTOC consists of a fibrillar material within which the axonemes are inserted. The Mt arrays that stiffen the axopods are thin (50–100 Mts in each) and radiate from the upper hemisphere of the MTOC, whereas the rods in the stalk are much larger (500–2000 Mts per rod) and lie parallel to one another. The MTs are straight and continuous from the head to the base (Fig. 7 *a*). Within each rod the microtubules are arranged in a hexagonal pattern (Fig. 7 *c*).

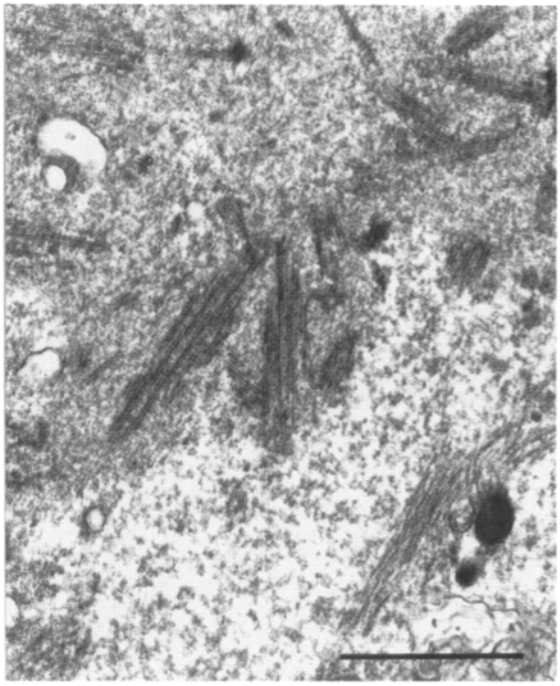

Figure 8. Cross-section through the base just after rapid contraction in SW showing small short segments of axonemes that are randomly distributed in a granular background substance. Bar, 1 μm.

Microtubule Arrays after Rapid Contraction Elicited by Stimulation

After rapid contraction in SW, the axopods, stalk, and head are no longer distinguishable and the cell body has become conical or flattened. However, the MTOC remains obvious even in the light microscope. Thin sections through the base of individuals that have been fixed immediately after stimulation show large areas which result from axoneme disassembly. The axonemes are incompletely dissociated. Instead of being radially arranged as in the extended form, they appear as short segments randomly scattered in the region of the MTOC which consists now of an area of granular material (Fig. 8).

Mt Arrays after Mild Destabilization

In specimen fixed during the slow contraction, longitudinal thin sections through the stalk, and the axopods show long regions where the Mt rods are parallel to one another, interrupted by one or a series of transversal areas consisting of a granular material (Fig. 9, *a–c*). These areas, called destabilization bands (DBs), appear to be more or less regularly distributed. According to their orientation to the long axis of the axoneme, three types of DBs can be seen: normal, oblique, or chevron shaped. The normal and oblique bands (0.1–0.4-μm long) are found in the axopodia and the single stalk of young individuals. The chevron-shaped bands are found in the stalk of large individuals stiffened with multiple axonemes. They are in groups of 6–20 making a zig-zag pattern and their thickness is irregular (Fig. 9 *a*). Between the successive DBs the orientation of the Mt segments are sightly tilted with regard to the general orientation of the Mt bundle (Fig. 9 *b*). In cross sections, the Mt arrays are embedded in the dense granular material of the DBs. All of these DBs are composed of closely packed granules (Fig. 9, *b* and *c*). They appear to be randomly distributed but granules are often aligned forming short rectilinear or curved segments. On the edges of the axonemes some Mts appear to be disconnected from the others and broken. Diverse disassembly forms of Mts such as incomplete C-shaped Mts, granular areas that seem to include small polymers and helices are lying in the cytoplasm and the axopodia (Fig. 10, *a* and *b*). Such disassembly forms are particularly evident in the axopodia. In cross-sections the axonemes are more or less disorganized depending on the destabilization process (incubation medium, incubation time). The Mt rods are converted into whorls consisting of the alignment of short segments of Mt helices that lie parallel with each other suggesting that the axopodia were curling or swirling down while the fixation occurred.

Discussion

In the stalked heliozoan *A. contractilis*, the rapid contraction of a transient axopodial system (axopods and stalk) is precisely correlated with the very dynamic destabilization of a prominent Mt-based cytoskeleton. At the initial state (extended specimen) the Mts are cross-connected by MAPs and capped by their proximal ends (minus ends) on a single MTOC. They are nearly all of the same length (spike distribution) and uninterrupted. In the just contracted state the Mts are almost totally disconnected and disassembled. The transition between these two states in conditions close to the natural environment (without using treatments suspected to modify Mt behavior) proceeds as a quasi-explosive phase. Our observations based on real time analysis of the shortening in natural and articial conditions coupled with ultrastructural data, suggest that intercalary destabilization and breakdown followed by Mt disassembly take place during contraction. This process may be emphasized by a very rapid transformation of Mts into helical forms of partially disassembled Mt protofilaments.

The Equivalence of the Slowed Process with the Rapid Undisturbed Process

Slowing the movement with AMs or drugs had two advantages. First, it allowed us to slow the Mt disassembly process and to visualize the cell shape change with videoscopy. Secondly, it is the only way chemical fixations for EM can be made in the course of the Mt destabilization, as the effect of the fixative is slower than the natural rapid contraction itself.

Although they have different targets, all the AMs used to effect complete or mild destabilization of the Mt arrays (those intervening directly on the Mts or those acting on calcium pathways) produced similar slowing effects which were rapidly reversed after rinsing in SW. The ultrastructural aspect of the Mt bundles was similar whatever the stabilization procedures, provided that osmolarity, ionic strength, and pH were around those found in SW.

As already observed (Marsland et al., 1971; Sato et al., 1984), deuterium oxide induces stabilization of the Mt-arrays. Heavy water may produce viscous interactions with the cytoplasmic structures and in *Actinocoryne* it allowed us to fix the extended specimens for EM without modifying the aspect of the Mt cytoskeleton.

Since Mt disassembly is promoted by cytosolic uptake of

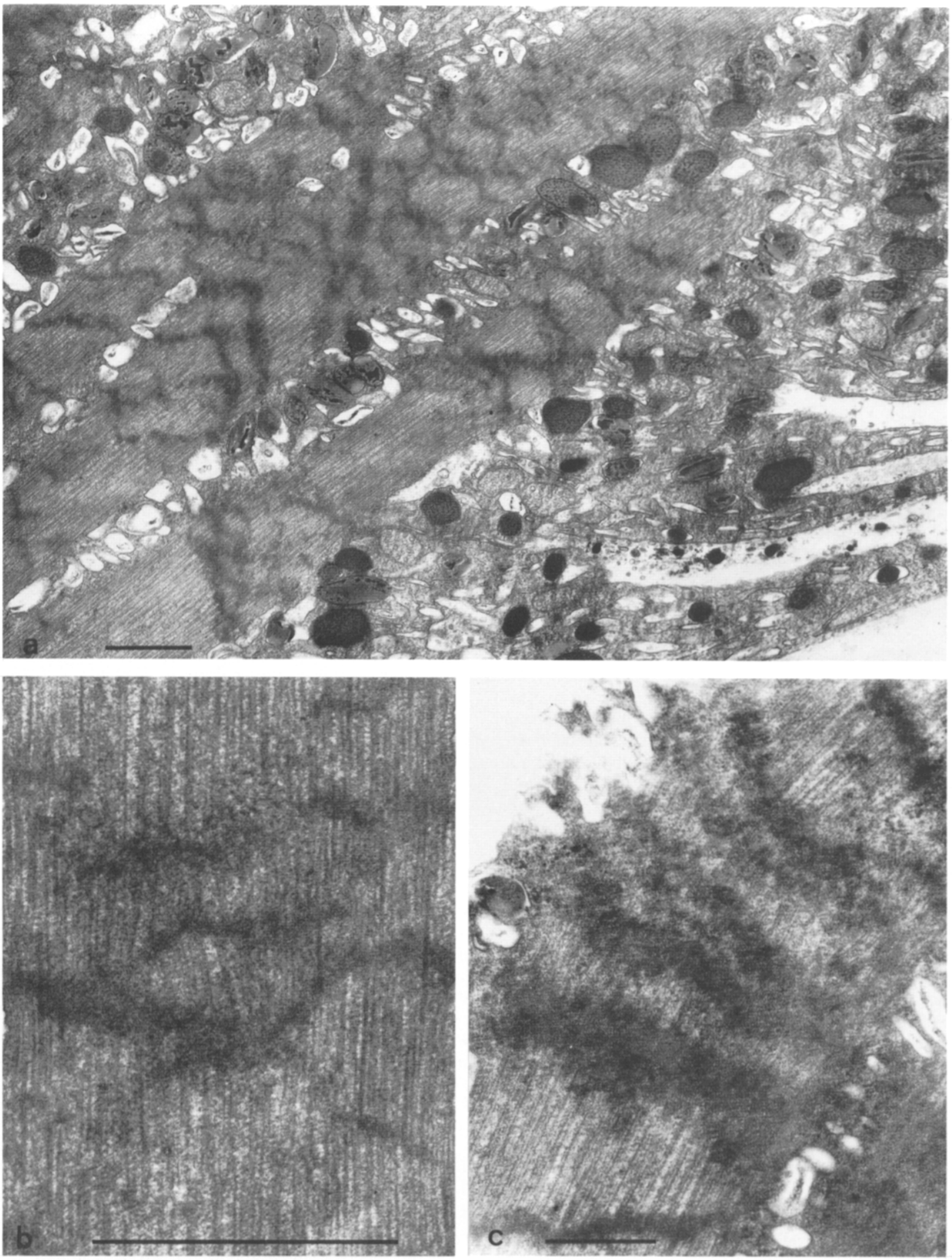

Figure 9. Longitudinal thin section through axonemes of a specimen submitted to mild destabilizing AM containing 500 mM Tris, 10 mM KCl, 1.5 mM $CaCl_2$, 2 mM EGTA, for 10 min before fixation (no EGTA was added into the fixative) showing the destabilization bands. (*a*) Numerous chevron-shaped DBs are seen in the three parallel Mt rods. (*b*) Detail of the chevron-shaped pattern showing that the Mts are tilted between successive DBs. (*c*) A series of DBs in the folded region of the stalk showing the enlargement of this region which resembles a knee as shown on Fig. 5. The Mt arrays are interrupted by several DBs. Bars, 1 μm.

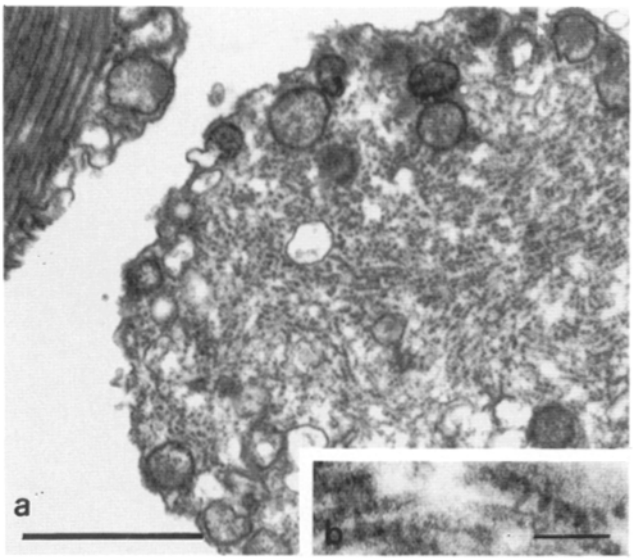

Figure 10. Tubulin polymorphism viewed after mild destabilization in AM containing 500 mM Tris, 10 mM KCl, 10 mM $MgCl_2$, 1 mM EGTA, pH 6.2 for 4 min. (*a*) Cross section through an axopod during the slowed contraction showing tubulin helices. (*b*) Longitudinal thin section through a tubulin helix at high magnification. Bars: (*a*) 1 μm; (*b*) 0.1 μm.

Ca^{2+}, it is likely that the delayed and slowed contraction often observed in Ca^{2+}-free AMs ($\sim 10^{-8}$–10^{-7} M) or in the presence of inhibitors of Ca^{2+} pathways (Ca^{2+} channel blockers, caffeine, quercetine) may be caused by Ca^{2+} release from internal Ca^{2+} stores.

Both the rapid contraction in SW and the slowed contraction in AMs followed exponential kinetics but half time of the rapid contraction is 4 ms (apparent dissociation rate 3.10^7 subunits/s) whereas half time of the slowed motion is ~3 s (disassembly rate 3,000–4,000 dimers/s). At the beginning of the event only the tubulin dimers from the DBs are scattered into the cytoplasm, whereas at the end of the process nearly the whole axonemal system is converted into granular material.

The exact similarity in the shape of the rapid and the slowed contractions, the fact that the curves are decreasing exponentials exhibiting small breaks in the slope, the presence of fragments of axonemes in the base of just contracted specimens and of dissociation areas in the axonemes of specimens fixed during the slowed contraction, strongly suggest that a process of intercalary disassembly and breakdown occurs during the rapid and the slowed contractions and that both contractions are equivalent. Therefore, we consider that the results obtained from the slowed contraction induced in AMs are useful to understand such a rapid destabilization of microtubules.

The In Vivo Demonstration of Breakage

A mechanism of fragmentation may account for the rapid cell shortening as suggested by the following observations: (*a*) The presence of slightly jerky contractions, foldings, and breaks as seen in high speed films, events which may correspond to the small ruptures of the slope in the curves of length change versus time; (*b*) in the extended specimens (viewed in polarized light or in thin sections), the Mt cytoskeleton is straight and continuous, whereas it is fragmented and almost completely dissociated after contraction; and (*c*) the contraction velocity elicited in conditions close to the natural environment (without using treatments suspected to modify Mt behavior) proceeds at ms range. A comparison with disassembly rates in in vitro conditions or in other cell types (where endwise depolymerization has been reported) displays the distinctiveness of *Actinocoryne* concerning Mt shortening. The maximum number of tubulin dimers lost per second is ~4,500 in in vitro Mts at steady state (Caplow et al., 1988). It is much slower (992 dimers/s) in the non-kinetochorial Mts previously blocked with antimitotic drugs (Salmon et al., 1984*a*). It comprises between 300 and 500 dimers/s in cytoplasmic Mts of diverse cells (Salmon et al., 1984*b*; Cassimeris et al., 1986, 1988; Wadsworth and Salmon, 1988) and it is only 116 dimers/s in fibroblasts (Sammak et al., 1987). In contrast, the mean half time of 4 ms for the rapid contraction in *Actinocoryne* reveals an apparent Mt disassembly rate of 3.10^7 subunits per s, i.e., at the least 10^4 times larger than in other systems.

Kinetics of Mt Shortening in Actinocoryne

As in many other biological phenomena, shortening of the axopodial system in *Actinocoryne* follows decreasing exponential kinetics and in natural or artificial media the curves of the length change versus time are either smooth or proceed by successive steps. This is not in agreement with the model of Kristofferson and co-workers (1980) who showed that for a spike distribution of Mt lengths, the rate of shortening is linear rather than exponential. However, these authors examined the depolymerization kinetics of Mts reconstituted from purified MAP-free tubulin. One can expect that the kinetics of disassembly for a complex system of Mts in intact living cells (tightly connected by MAPs, capped on a MTOC and interacting with other cytoplasmic components) do not correspond to a theoretical model resulting from in vitro experiments performed in strictly controlled conditions. If numerous breaks take place within a very short delay, as is presumably the case during the rapid contraction, many segments are produced whose length distribution may be consistent with exponential decrease. The small ruptures of the slope in the curves of length change versus time may be interpreted as slight changes in the kinetics corresponding to some stops in the breakage events. To support this hypothesis we tried to determine the length distribution of the segments during cell shortening but our preparations of spread axonemes have been unsuccessful. Reconstitution of the distribution of lengths from serial sections through specimens cryosubstituted at diverse times during the natural or slowed contractions and immunolabeling coupled to confocal microscopy may provide additional information.

Electron Microscopical Evidence for Intercalary Destabilization and Mt Breakdown

Serial longitudinal sections through mildly destabilized specimens provided the strongest argument for the hypothesis of intercalary destabilization and fragmentation. Granular areas are intercalated between short segments of slightly tilted Mts and suggest that they consist of DBs resulting from intercalary disassembly of the Mt arrays. Since they are

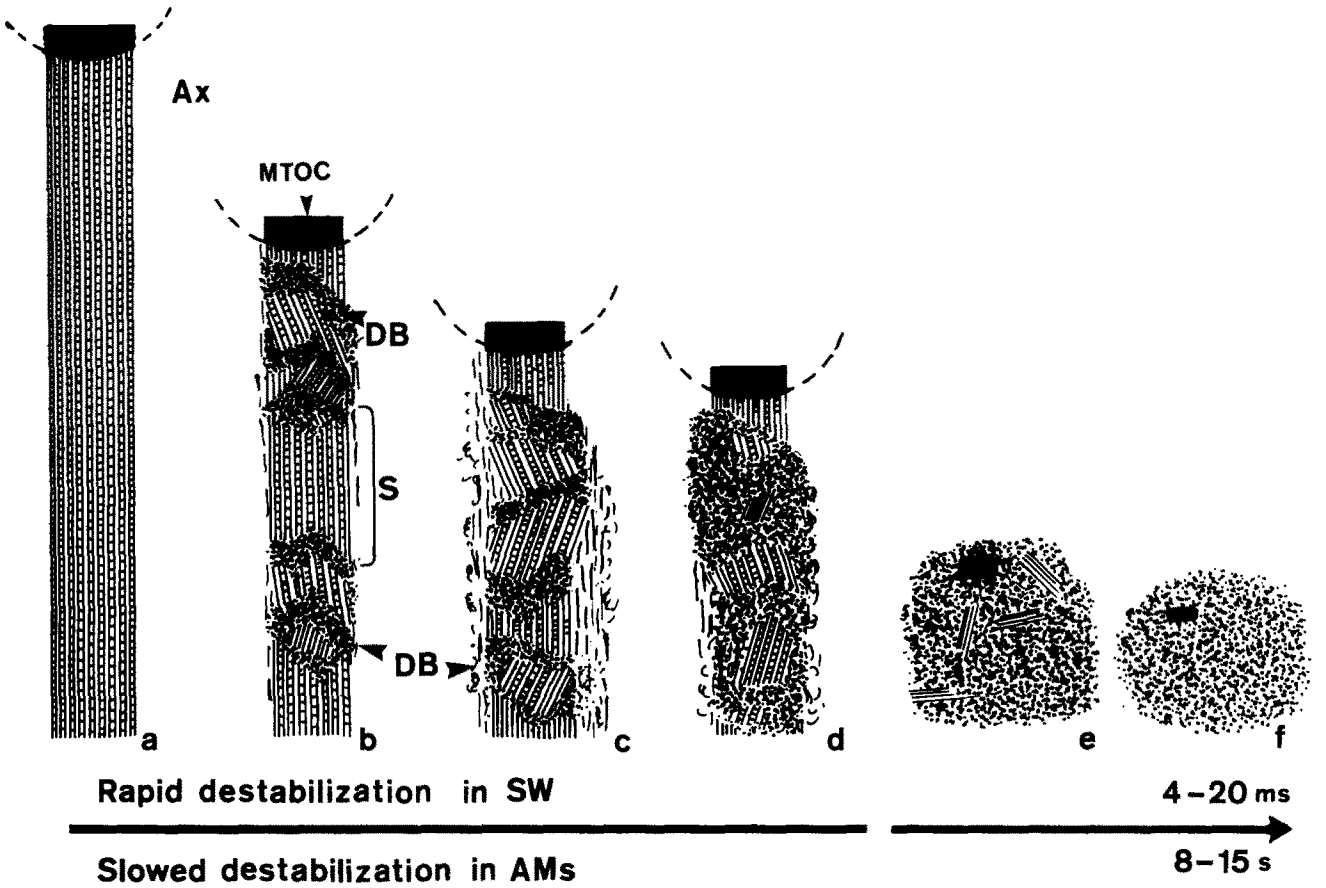

Figure 11. Interpretative drawing of a possible sequence of intercalary disassembly, breakdown and formation of polymorphic forms of Mt disassembly in the axonemal system (*Ax*, axoneme; *MTOC*, microtubule organizing center) during contraction of the stalk in *Actinocoryne*. Rapid destabilization in SW takes place within 4–20 ms (upper part of the horizontal time scale). Slowed destabilization in AMs occurs within 8–15 s (lower part of the horizontal time scale). (*a*) Intact axoneme consisting of Mts cross connected by bridges arising from a single MTOC. (*b*) Initial step of intercalary destabilization and breakdown of the axoneme showing destabilization bands (*DB*) between almost intact Mt arrays. In the DBs both Mts and MAPs are converted into small polymers within a granular material. Between the successive DBs the orientation of the Mt segments (*S*) are slightly tilted with regard to the general orientation of the Mt bundle. On the edges of the axoneme, the Mts are disconnected and broken. (*c*) The segments are shorter and the DBs larger. In the cytoplasm, diverse disassembly forms of Mts such as linear and helical polymers are seen. (*d*) The process of Mt-disassembly goes on. (*e*) Some tiny segments, randomly scattered throughout the granular substance are still visible after contraction. (*f*) At the end of the process the Mt segments are invisible. Only a few short single Mts are visible around the MTOC.

never observed in the fully stabilized specimens, the DBs may not be intrinsic or artifactual features generated by some uncontrolled effect of the stabilization or the fixation treatments. In contrast, they are only seen in the mildly destabilized specimens whatever the stabilization and fixation techniques. As such DBs were found in longitudinal, oblique, or cross sections, their presence is independent of the sectioning angle. The presence of DBs extending the whole width of the axoneme suggests that destabilization sites in one Mt coincide with those in the neighboring Mts and supports the hypothesis that destabilization occurs synchronously for all of the Mts in the axoneme. The vibrations or the oscillations of the stalk during contraction may correspond to successive breaks in the Mt bundles and may explain why a single or multiple DBs can be seen in thin sections depending upon fixation time. These DBs may be considerably more numerous and thinner in the rapid contraction elicited in natural conditions than in AMs. It is likely that the less stabilized the cell is, the more numerous are the DBs. The presence of Mts partially disconnected from the edges of the rods, and of segments and diverse disassembly forms of tubulin in the adjoining cytoplasm indicates that lateral disassembly may accompany the intercalary destabilization.

All of these observations suggest that the axonemes are disassembled in domains that are more fragile or unstable than in others. Whether these domains correspond to post-transcriptional tubulin heterogeneity, local cytoplasmic factors such as severing proteins or intercalary GTP-binding properties is unknown. The recent discovery of severing proteins in *Xenopus* eggs (Vale, 1991) suggests that disassembly of *Actinocoryne* axonemes may also take place via a similar pathway.

A Possible Mechanism of Rapid Mt Disassembly

The endwise disassembly mechanism cannot account for the very rapid disassembly process seen in natural conditions. If Mt shortening proceeded in *Actinocoryne* by endwise depolymerization only, using a plausible apparent dissociation rate constant of 3.10^3 dimers per second and per Mt of 150-

μm long (based on 1,625 dimers per μm), the phenomenon would last 81 s.

If fragmentation is responsible (taken the above dissociation rate constant and the half time of 4 ms), the Mts would have been fragmented in 10^4 segments each containing 24 subunits. Since the apparent constant dissociation rate in *Actinocoryne* is 3.10^7 dimers $\cdot s^{-1}$ (i.e., 10^4 times larger) one may suggest that the axopodial rod is fragmented along its whole length and converted into diverse tubulin disassembly forms, especially whorls of tubulin helices (Fig. 10 *a*). This transformation may increase the destabilization velocity as recently suggested by Chen and Schliwa (1990) for the rapid Mt disassembly in *Reticulomyxa*. It is likely that similar processes of Mt disassembly may occur in other heliozoans where measurement of axopodial contraction represents a loss of tubulin dimers 4–20 times slower than in *Actinocoryne* but still very rapid when compared with the other systems of unstable Mts (Davidson, 1975; Shigenaka et al., 1982).

Intercalary destabilization and breakdown appear to be a part of in vivo Mt disassembly in *Actinocoryne* and Fig. 11 shows a probable sequence of events with the following characteristics: (*a*) Cytosolic Ca^{2+} uptake resulting from stimulation (Ca^{2+} influx via Ca^{2+}- and Na^+-dependent action potential and/or Ca^{2+} release from internal Ca^{2+} stores); (*b*) activation of Ca^{2+}-dependent sensitive sites along the Mts; (*c*) formation of intercalary destabilization bands consisting of disassembled Mts and MAPs; and (*d*) transformation into diverse disassembly forms of Mts.

It is likely that strong tensile forces exist in the extended specimens which may be liberated suddenly by intercalary disassembly and breakdown of the axonemes. Whatever the possible implications for other cytoskeletal elements and regulatory processes, this sequence of intercalary Mt destabilization and breakdown may be a prerequisite allowing cell contraction to be driven.

We would like to thank Q. Bone and P. Chang for stimulating discussion and critical analysis of the manuscript. We are very grateful to all our colleagues from the "Groupe de Biologie Cellulaire Marine," especially C. Sardet for enthusiastic support.

Received for publication 24 July 1991 and in revised form 29 November 1991.

References

Caplow, M., J. Shanks, S. Breidenbach, and R. L. Ruhlen. 1988. Kinetics and mechanisms of microtubule length changes by dynamic instability. *J. Biol. Chem.* 263:10943–10951.

Carlier, M. F. 1982. Guanosine-5'-triphosphate hydrolysis and tubulin polymerization. *Mol. Cell Biochem.* 47:95–113.

Carlier, M. F., and D. Pantaloni. 1981. Kinetic analysis of guanosine 5'-triphosphate hydrolysis associated with tubulin polymerisation. *Biochemistry.* 20:1918–1924.

Cassimeris, L., N. K. Pryer, and E. D. Salmon. 1988. Real-time observations of microtubule dynamic instability in living cells. *J. Cell Biol.* 107:2223–2231.

Cassimeris, L., P. Wadsworth, and E. D. Salmon. 1986. Dynamics of microtubule depolymerization in monocytes. *J. Cell Biol.* 102:2023–2032.

Chang, D., P. S. Hsieh, and D. C. Dawson. 1988. Calcium: a program in basic for calculating the composition of solutions with specified free concentrations of calcium, magnesium and other divalent cations. *Comput. Biol. Med.* 18:351–366.

Chen, Y.-T., and M. Schliwa. 1990. Direct observation of microtubule dynamics in *Reticulomyxa*: unusually rapid length changes and microtubule sliding. *Cell Motil. Cytoskeleton.* 17:214–226.

Davidson, L. A. 1975. Studies of the actinopods *Heterophrys marina* and *Ciliophrys marina*: energetics and structural analysis of their contractile axopodia. General ultrastructure and phylogenetic relationships. PhD Thesis, University of California, Berkeley. 1–163.

De Brabander, M. J., R. M. L. van de Veire, F. E.M. Aerts, M. Borgers, and P. A. J. Janssen. 1976. The effect of methyl(5-2 thyenyl carbonyl)1H. Benzimidazol 2phenyl carbamate (R 17934 HSC 238159) a new system antitumoral drug interfering with microtubules on mammalian cells cultured *in vitro*. *Cancer Res.* 36:905–916.

Febvre-Chevalier, C. 1980. Behavior and cytology of *Actinocoryne contractilis*, nov. gen. nov. sp. A new stalked heliozoan (Centrohelidia). Comparison with the other related genera. *J. Mar. Biol. Ass. U.K.* 60:909–928.

Febvre-Chevalier, C. 1981. Preliminary study of the motility processes in the stalked heliozoan *Actinocoryne contractilis*. *Biosystems.* 14:337–343.

Febvre-Chevalier, C. 1989. Phylum Actinopoda Class Heliozoa. *In* Handbook of Protoctists. L. Margulis, J. O. Corliss, M. Melkonian, and D. Chapman, editors. Jones and Bartlett Inc., Boston, MA. 20b:347–362.

Febvre-Chevalier, C., A. Bilbaut, Q. Bone, and J. Febvre. 1986. Sodium-calcium action potential associated with contraction in the heliozoan *Actinocoryne contractilis*. *J. Exp. Biol.* 122:177–192.

Febvre-Chevalier, C., and J. Febvre. 1981. Cytophysiology of motility in a stalked heliozoan. Film SFRS, Paris.

Febvre-Chevalier, C., and J. Febvre. 1986. Motility mechanisms in the actinopods (Protozoa): a review with particular attention to axopodial contraction/extension and movement of nonactin filament systems. *Cell Motil. Cytoskeleton.* 6:198–208.

Inoué, S., and H. Ritter. 1975. Dynamics of mitotic spindle organization and function. *In* Molecules and Cell Movement. S. Inoué and R. E. Stephens, editors. Raven Press, New York. 3–30.

Inoué, S., and H. Sato. 1967. Cell motility by labile association of molecules. *J. Gen. Physiol.* 50:259–292.

Johnson, K. A., and G. G. Borisy. 1977. Kinetic analysis of microtubule self-assembly *in vitro*. *J. Mol. Biol.* 177:1–31.

Kristofferson, D., T. L. Karr, and D. L. Purich. 1980. Dynamics of linear polymer disassembly. *J. Biol. Chem.* 255:8567–8572.

Marsland, D., L. G. Tilney, and M. Hirshfield. 1971. Stabilizing effect of heavy water on the microtubular components and needle-like form of the heliozoan axopods: a pressure temperature analysis. *J. Cell Physiol.* 77:187–194.

Mitchison, T., and M. Kirschner. 1984. Dynamic instability of microtubule growth. *Nature (Lond.).* 312:237–242.

Salmon, E. D. 1984. Tubulin dynamics in microtubules of the mitotic spindle. *In* Molecular biology of the cytoskeleton. G. G. Borisy, D. W. Cleveland, and D. B. V. Murphy. Cold Spring Harbor Laboratory Press, Cold Spring Harbor, NY. 99–109.

Salmon, E. D., R. J. Leslie, W. M. Saxton, M. L. Karow, and J. R. McIntosh. 1984*a*. Spindle microtubule dynamics in sea urchin embryos: analysis using a fluorescein-labeled tubulin and measurements of fluorescent redistribution after laser photobleaching. *J. Cell Biol.* 99:2165–2174.

Salmon, E. D., M. McKehl, and T. Hays. 1984*b*. Rapid rate of tubulin dissociation from microtubules in the mitotic spindle in vivo measured by blocking polymerization with colchicine. *J. Cell Biol.* 99:1066–1075.

Sammak, P. J., G. J. Gorbsky, and G. G. Borisy. 1987. Microtubule dynamics in vivo: a test of mechanisms of turnover. *J. Cell Biol.* 104:395–405.

Sato, H., T. Kato, C. Takahashi, and T. Ito. 1982. Analysis of D_2O effect on *in vivo* and *in vitro* tubulin polymerization and depolymerisation. *In* Biological Function of Microtubules and Related Structures. H. Sakai, H. Mohri, and G. G. Borisy, editors. Academic Press, New York. 20:211–224.

Shigenaka, Y., K. Yano, R. Yogosawa, and T. Suzaki. 1982. Rapid contraction of the microtubule containing axopodia in a large heliozoan *Actinosphaerium*. *In* Biological Functions of Microtubules and Related Structures. H. Sakai, H. Mohri, and G. G. Borisy, editors. Academic Press, New York. 105–114.

Tilney, L. G., and K. R. Porter. 1965. Studies on the microtubules in Heliozoa. I. Fine structure of *Actinosphaerium* with particular reference to axial rod structure. *Protoplasma.* 60:317–344.

Tilney, L. G., and K. R. Porter. 1967. Studies on the microtubules in Heliozoa. II. The effects of low temperature on these structures in the formation and maintenance of the axopodia. *J. Cell Biol.* 34:327–343.

Vale, R. D. 1991. Severing of stable microtubules by a mitotically activated protein in *Xenopus* egg extracts. *Cell.* 64:827–839.

Wadsworth, P., and E. D. Salmon. 1988. Spindle microtubule dynamics: modulation by metabolic inhibitors. *Cell Motil. Cytoskeleton.* 11:97–105.